Article

Single-Conformation Ultraviolet and Infrared Spectroscopy of Model Synthetic Foldamers: β-Peptides Ac-β-hPhe-NHMe and Ac-β-hTyr-NHMe

Esteban E. Baquero, William H. James, Soo Hyuk Choi, Samuel H. Gellman, and Timothy S. Zwier

J. Am. Chem. Soc., **2008**, 130 (14), 4784-4794 • DOI: 10.1021/ja078271y

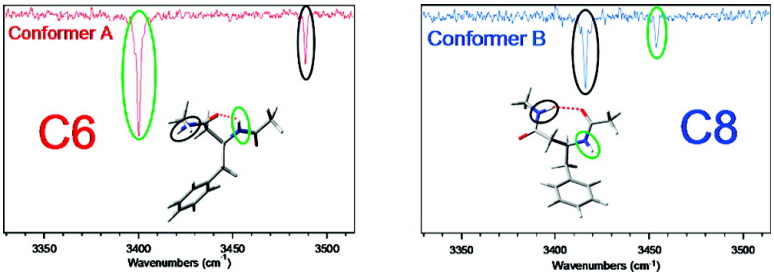

More About This Article

Additional resources and features associated with this article are available within the HTML version:

- Supporting Information
- Links to the 4 articles that cite this article, as of the time of this article download
- Access to high resolution figures
- Links to articles and content related to this article
- Copyright permission to reproduce figures and/or text from this article

View the Full Text HTML

J|A|C|S
ARTICLES
Published on Web 03/18/2008

Single-Conformation Ultraviolet and Infrared Spectroscopy of Model Synthetic Foldamers: β-Peptides Ac-β^3-hPhe-NHMe and Ac-β^3-hTyr-NHMe

Esteban E. Baquero,[†] William H. James, III,[†] Soo Hyuk Choi,[‡] Samuel H. Gellman,[‡] and Timothy S. Zwier*,[†]

Department of Chemistry, Purdue University, West Lafayette, Indiana 49707-2084, and Department of Chemistry, University of Wisconsin, Madison, Wisconsin 53706

Received October 29, 2007; E-mail: zwier@purdue.edu

Abstract: The conformational preferences and infrared and ultraviolet spectral signatures of two model β-peptides, Ac-β^3-hPhe-NHMe (**1**) and Ac-β^3-hTyr-NHMe (**2**), have been explored under jet-cooled, isolated molecule conditions. The mass-resolved, resonant two-photon ionization spectra of the two molecules were recorded in the region of the S_0-S_1 origin of the phenyl or phenol ring substituents, respectively. UV−UV hole-burning spectroscopy was used to determine that two conformations of **1** are present, with the transitions due to conformer A, with S_0-S_1 origin at 34431 cm^{-1}, being almost 20 times larger than those due to conformer B, with S_0-S_1 origin at 34404 cm^{-1}. Only one conformation of **2** was observed. Resonant ion-dip infrared spectroscopy provided single-conformation infrared spectra in the 3300−3700 cm^{-1} region. The spectra of conformer A of both molecules have H-bonded and free amide NH stretch infrared transitions at 3400 and 3488 cm^{-1}, respectively, while conformer B of **1** possesses bands at 3417 and 3454 cm^{-1}. For comparison with experiment, full optimizations of all low-lying minima of **1** were carried out at the DFT B3LYP/6-31+G* and RIMP2/aug-cc-pVDZ levels of theory, and single point MP2/6-31+G* calculations at the DFT geometries. On the basis of the comparison with previous studies in solution and the calculated results, conformer A of **1** and **2** were assigned to a C6 conformer, while conformer B of **1** was assigned to a unique C8 structure with a weak intramolecular H-bond. The reasons for the preference for C6 over C8 structures and the presence of only two conformations in the jet-cooled spectrum are discussed in light of the predictions from calculations.

1. Introduction

In recent years, there has been a surge of interest in exploring the properties of synthetic foldamers, that is, oligomers made up of building blocks that differ in well-defined ways from the α-amino acid units that comprise natural proteins.[1−5] The use of unnatural subunits in place of α-amino acid residues gives foldamer backbones unique secondary and tertiary structural possibilities. Foldamers are of possible practical interest because they can display useful chemical[6] and biological[7] activities.

One class of synthetic foldamers that has generated particular interest and attention are β-peptides,[8−11] which differ from α-peptides in having two carbon atoms rather than one linking adjoining amide groups. This additional carbon adds flexibility to the polypeptide backbone and changes the relative spacing between amide groups. This backbone variation changes the nature of the amide−amide H-bonds that dictate the propensity toward helical or other secondary structures, relative to proteins. These preferences can be fine-tuned by changing substituents at the β^2 and/or β^3 position.[10,11]

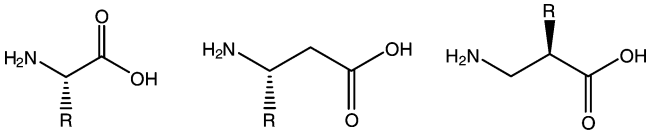

α-amino acid β^3-amino acid β^2-amino acid

The fundamental base of knowledge regarding the inherent conformational preferences and potential energy landscapes of β-peptides is much less developed than that of α-peptides. One useful strategy to address this deficiency is to study the conformational preferences through conformation-specific spectroscopy of isolated β-peptides free from solvent. In this way,

[†] Purdue University.
[‡] University of Wisconsin.

(1) Gellman, S. H. *Acc. Chem. Res.* **1998**, *31*, 173−180.
(2) Kirshenbaum, K.; Zuckermann, R. N.; Dill, K. A. *Curr. Opin. Struct. Biol.* **1999**, *9*, 530−535.
(3) Hill, D. J.; Mio, M. J.; Prince, R. B.; Hughes, T. S.; Moore, J. S. *Chem. Rev.* **2001**, *101*, 3893−4011.
(4) Huc, I. *Eur. J. Org. Chem.* **2004**, 17−29.
(5) Hecht, S.; Huc, I. *Foldamers: Structure, Properties, and Applications*; Wiley-VCH: Weinheim, 2007.
(6) Pomerantz, W. C.; Abbott, N. L.; Gellman, S. H. *J. Am. Chem. Soc.* **2006**, *128*, 8730−8731.
(7) Goodman, C. M.; Choi, S.; Shandler, S.; DeGrado, W. F. *Nat. Chem. Biol.* **2007**, *3*, 252.
(8) Dado, G. P.; Gellman, S. H. *J. Am. Chem. Soc.* **1994**, *116*, 1054−1062.
(9) Seebach, D.; Matthews, J. L. *Chem. Commun.* **1997**, 2015−2022.
(10) Cheng, R. P.; Gellman, S. H.; DeGrado, W. F. *Chem. Rev.* **2001**, *101*, 3219−3232.
(11) Seebach, D.; Beck, A. K.; Bierbaum, D. J. *Chem. Biodivers.* **2004**, *1*, 1111−1239.

10.1021/ja078271y CCC: $40.75

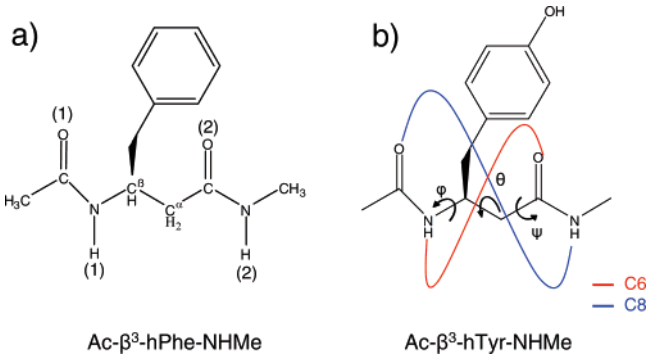

Figure 1. Structures for (a) 3-acetoamido-*N*-methyl-4-phenylbutamide (Ac-β^3-hPhe-NHMe, **1**) and (b) 3-acetamido-4-(4-hydroxyphenyl)-*N*-methylbutamide (Ac-β^3-hTyr-NHMe, **2**). (a) The numbers in parentheses indicate the labeling scheme used for the amide groups along the peptide chain. (b) The indicated curves connect NH and C═O groups that can be involved in intramolecular H-bonds. The indicated angles are the relevant Ramachandran angles used to conduct conformational searches in β-peptides.

the inherent conformational preferences can be determined and their spectral signatures explored. This strategy has been used to good advantage in previous work on α-peptides, probing in some detail their single-conformation spectroscopy up through tetra-, pentapeptides, and beyond.[12−22] Many of these studies incorporate an aromatic chromophore that enables double resonance spectroscopy to determine the number of conformations present and obtain their ultraviolet and infrared spectral signatures. The amide NH stretch region of the infrared was used as a powerful diagnostic of the H-bonded architectures present in these molecules. The number and strength of the H-bonds are imprinted on the NH stretch fundamentals, producing shifts in vibrational frequency and enhancements in infrared intensity that are diagnostic of the structure. Assignments have been made to various peptide backbone conformations, including structures that incorporate 5-membered (C5), 7-membered (C7), and 10-membered (C10) H-bonded rings.

In this paper, we extend such studies to two model β-peptides containing either a phenylalanine or tyrosine side chain. 3-Acetoamido-*N*-methyl-4-phenylbutamide (Ac-β^3-hPhe-NHMe, **1**) and 3-acetamido-4-(4-hydroxyphenyl)-*N*-methylbutamide (Ac-β^3-hTyr-NHMe, **2**) contain a single β-amino acid residue (Figure 1), which has the flexibility to accommodate two types of intramolecular hydrogen-bonded structures, shown in Figure 1b. A six-membered cycle (C6) can form when the N−H of the N-terminal amide (NH(1)) acts as donor in a H-bond with the oxygen of the C-terminal carbonyl group (CO(2)). This leaves the C-terminal NH(2) group free. Alternatively, an eight-membered cycle (C8) can form when the N−H of the C-terminal amide (NH(2)) hydrogen bonds to the C═O of the N-terminal amide (CO(1)), leaving NH(1) free. As we shall see, these model β-peptides show evidence for both H-bonded motifs, with the C6 ring being dominant.

There is one previous report on the gas-phase rotational spectroscopy of β-alanine,[23] which finds evidence for a C6 conformer analogous to that just described. There are several studies of small model β-peptides in dilute, nonpolar solution, where many of the same issues regarding the inherent conformational preferences of the β-peptides were explored.[8,24,25] The results from Marraud and co-workers[25] and Dado and Gellman[8] are of most direct relevance, since both groups used amide NH stretch infrared spectra as a tool in assigning the observed conformations. In particular, Marraud et al.[25] compared the IR spectra of *N*-acetyl-3-aminobutanoic acid-*N*′-methylamide (Ac-β^3-hAla-NHMe, **3**), which contains a branched-chain β^3 carbon, with Ac-β-hGly-NHMe (**4**), in which β^3 carbon is unbranched.

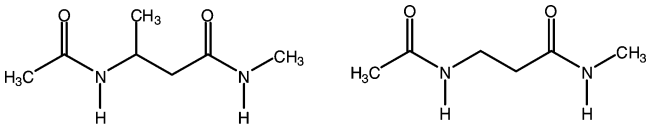

3 **4**

These authors assigned bands in the amide NH stretch region to both C6 and C8 conformers. A key aspect of their assignment is their recognition that the free amide NH stretch bands can be used as a diagnostic of which group is *not* involved in the intramolecular H-bond. In **4**, both amide NH groups are attached to unbranched carbons, producing a single peak in the free amide NH stretch region. However, in **3**, two bands appear, with the free amide NH stretch of the branched chain lower in frequency than that of the NHMe group by ∼30−40 cm^{-1}. Since **1** differs from **3** only by addition of the phenyl group to the β^3 methyl substituent, we anticipate being able to use the same diagnostic in the present study. Indeed, we shall see that the positional dependence of the free amide NH stretch does carry over to isolated molecule conditions and can be used as an unequivocal signature distinguishing C6 from C8 cycles.

In support of our experimental work, we also carry out an extensive set of density functional theory and *ab initio* calculations of the structures, relative energies, vibrational frequencies, and infrared intensities of the various conformational minima of Ac-β^3-hPhe-NHMe. These calculations build closely on the results of previous calculations of Hofmann and co-workers[26,27] on **3**, which revealed several unique C6 and C8 conformers. These authors explored the conformational surface by systematically changing dihedral angles along the peptide backbone (ϕ, θ, ψ defined in Figure 1b) and optimizing the resultant structures

(12) Abo-Riziq, A. G.; Bushnell, J. E.; Crews, B.; Callahan, M. P.; Grace, L.; De Vries, M. S. *Int. J. Quantum Chem.* **2005**, *105*, 437−445.
(13) Abo-Riziq, A.; Bushnell, J. E.; Crews, B.; Callahan, M.; Grace, L.; De Vries, M. S. *Chem. Phys. Lett.* **2006**, *431*, 227−230.
(14) Abo-Riziq, A.; Crews, B. O.; Callahan, M. P.; Grace, L.; de Vries, M. S. *Angew. Chem., Int. Ed.* **2006**, *45*, 5166−5169.
(15) Chin, W.; Compagnon, I.; Dognon, J. P.; Canuel, C.; Piuzzi, F.; Dimicoli, I.; von Helden, G.; Meijer, G.; Mons, M. *J. Am. Chem. Soc.* **2005**, *127*, 1388−1389.
(16) Chin, W.; Dognon, J. P.; Canuel, C.; Piuzzi, F.; Dimicoli, I.; Mons, M.; Compagnon, I.; von Helden, G.; Meijer, G. *J. Chem. Phys.* **2005**, *122*.
(17) Chin, W.; Dognon, J. P.; Piuzzi, F.; Dimicoli, I.; Mons, M. *Mol. Phys.* **2005**, *103*, 1579−1587.
(18) Chin, W.; Mons, M.; Dognon, J. P.; Mirasol, R.; Chass, G.; Dimicoli, I.; Piuzzi, F.; Butz, P.; Tardivel, B.; Compagnon, I.; von Helden, G.; Meijer, G. *J. Phys. Chem. A* **2005**, *109*, 5281−5288.
(19) Chin, W.; Piuzzi, F.; Dimicoli, I.; Mons, M. *Phys. Chem. Chem. Phys.* **2006**, *8*, 1033−1048.
(20) Compagnon, I.; Oomens, J.; Meijer, G.; von Helden, G. *J. Am. Chem. Soc.* **2006**, *128*, 3592−3597.
(21) Reha, D.; Valdes, H.; Vondrasek, J.; Hobza, P.; Abu-Riziq, A.; Crews, B.; de Vries, M. S. *Chem.−Eur. J.* **2005**, *11*, 6803−6817.
(22) Dian, B. C.; Longarte, A.; Mercier, S.; Evans, D.; Wales, D. J.; Zwier, T. S. *J. Chem. Phys.* **2002**, *117*, 10688−10702.
(23) McGlone, S. J.; Godfrey, P. D. *J. Am. Chem. Soc.* **1995**, *117*, 1043−1048.
(24) Gellman, S. H.; Dado, G. P.; Liang, G. B.; Adams, B. R. *J. Am. Chem. Soc.* **1991**, *113*, 1164−1173.
(25) Marraud, M.; Neel, J. *J. Polym. Sci. Part C: Polym. Symp.* **1975**, *52*, 271−282.
(26) Mohle, K.; Gunther, R.; Thormann, M.; Sewald, N.; Hofmann, H. J. *Biopolymers* **1999**, *50*, 167−184.
(27) Gunther, R.; Hofmann, H. J. *Helv. Chim. Acta* **2002**, *85*, 2149−2168.

at the Hartree−Fock (HF) and density functional (B3LYP) levels of theory with two different basis sets (3-21G and 6-31G*). The optimization yielded a six-membered cycle (C6) as the lowest energy structure but also found several different types of C6 and C8 structures within a 20 kJ/mol energy window from the global minimum. These findings were later corroborated by Beke et al.[28,29] on the analogous β^3-monosubstituted peptide backbone without C-terminal methyl caps (HCO-β^3-hAla-NH_2). This study included optimizations at a higher level of theory (B3LYP/6-311++G(d,p)), which found the same C6 structure to be the global minimum. The higher level optimization also energetically rearranged structures above the global minimum and removed some higher energy C8 and extended structures that no longer formed stable minima.

In the present work, we extend these previous studies to completely explore the low-lying minima of **1**. It is important to note that the addition of the phenyl ring in **1** adds an extra degree of freedom which results in a larger number of conformers than in **3** or **4**.

Results from this study provide a foundation for experimental and theoretical exploration of the structures formed by larger β-peptides. This extension is taken up in the paper immediately following this one, where two larger phenyl-containing β-peptides are studied: Ac-β^3-hPhe-β^3-hAla-NHMe and Ac-β^3-hAla-β^3-hPhe-NHMe.[30] In these molecules, a rich variety of H-bonded structures are found, including single-ring (C10) and a variety of double-ring structures (C6/C6, C8/C8, and either C6/C8 or C8/C12).

2. Methods

2.1. Experiment. The synthesis and characterization of the β-peptide compounds studied followed well-established methods. The *N*-Boc protected β-amino acid methyl amides were prepared from the corresponding *N*-Boc-α-amino acids by a previously demonstrated, two-step procedure.[31] The α-amino acids were purchased from Novabiochem.

For the synthesis of Ac-β^3-hPhe-NHMe (**1**), Boc-β^3-hPhe-NHMe was treated with 4.0 M HCl in dioxane solution for 1 h. After evaporation of solvent, the hydrochloride salt was dissolved in aqueous $NaHCO_3$, and excess acetyl chloride was added with stirring. The reaction mixture was made basic to pH 8 with $NaHCO_3$, and the insoluble product was collected by suction filtration. The product was further purified by recrystallization from a methanol/ether/*n*-heptane mixture: ^{1}H NMR (300 MHz, CD_3OD) δ 7.33−7.11 (m, 5H), 4.41 (quintet, J = 6.5 Hz, 1H), 2.81 (ABX, J_{AB} = 13.4 Hz, J_{AX} = 6.1 Hz, J_{BX} = 7.8 Hz, $\Delta\upsilon$ = 0.07 ppm, 2H), 2.69 (s, 3H), 2.36 (ABX, J_{AB} = 13.8 Hz, J_{AX} = 5.7 Hz, J_{BX} = 6.9 Hz, $\Delta\upsilon$ = 0.05 ppm, 2H), 1.84 (s, 3H); ESI-TOF MS 235.4 $[M + H]^+$, 257.4 $[M + Na]^+$, 491.7 $[2M + Na]^+$.

The synthesis of Ac-β^3-hTyr-NHMe (**2**) involved an extra step relative to the synthesis of **1**. Ac-β^3-hTyr(OBn)-NHMe was synthesized from Boc-Tyr(OBn)-OH by a procedure analogous to that described above. The *O*-benzyl group was removed via hydrogenolysis with 10% palladium on activated carbon in methanol to yield the crude product, which was further purified by recrystallization from a methanol/ether/*n*-heptane mixture: ^{1}H NMR (300 MHz, CD_3OD) δ 7.02 (d, J = 7.5 Hz, 2H), 6.69 (, J = 7.5 Hz, 2H), 4.34 (quintet, J = 6.9 Hz, 1H), 2.78−2.62 (m, 3H), 2.33 (ABX, J_{AB} = 14.3 Hz, J_{AX} = 6.0 Hz, J_{BX} = 7.5 Hz, $\Delta\upsilon$ = 0.06 ppm, 2H), 1.85 (s, 1H); ESI-TOF MS 250.9 $[M + H]^+$, 272.8 $[M + Na]^+$, 522.7 $[2M + Na]^+$.

The experimental apparatus used in these studies has been described in detail elsewhere.[32] As a result, only a brief description will be given here. Ac-β^3-hPhe-NHMe (**1**) and Ac-β^3-hTyr-NHMe (**2**) were introduced into the gas phase by heating the sample to approximately 180−190 °C in a sample holder located directly behind a pulsed valve. A glass insert was placed inside a sample holder to minimize decomposition due to direct contact of the sample with the metal sample holder. The samples were expanded into vacuum via a pulsed valve (Parker General Valve, Series 9, 400 μm orifice, 20 Hz) using a 70/30 neon/helium gas mixture as a carrier gas with a backing pressure of 1.7 bar. The collisionally cooled molecules were interrogated in the ionization region of a time-of flight-mass-spectrometer (TOFMS) approximately 10 cm from the nozzle. The ionization and source regions are separated by a conical skimmer (Beam Dynamics, Inc., 55° conical angle, 2 mm diam). Flow rates of 0.15−0.30 bar•cm^3/s were maintained in order to avoid skimmer interference.

Electronic spectra were recorded by employing one-color-resonant two-photon ionization (R2PI), exciting the molecules with the frequency-doubled output of an Nd:YAG (Continuum) pumped tunable dye laser (Lambda-Physik Scanmate). The resultant ultraviolet radiation (0.1−0.5 mJ/pulse) traverses the ion source region of the TOFMS in a collimated beam of ∼1 mm diameter. The ions were detected by a microchannel plate detector (RM Jordan, 2.5 cm) mounted on top of a 1 m flight tube.

Conformation specific electronic spectra were obtained using UV−UV hole-burning (UVHB) spectroscopy. A higher power hole-burning laser (10 Hz) was fixed on a transition observed in the R2PI spectrum, and the probe laser (20 Hz) was scanned over the wavelength region of interest. The two laser beams were counter-propagated, spatially overlapped, and separated temporally so the hole-burning laser preceded the probe by 200 ns. The hole-burning spectra were recorded by monitoring, via active baseline subtraction, the difference between the ion signal due to the probe laser with the hole-burning laser "on" or "off". All bands that originate from the same ground state level as the transition on which the hole-burn laser is fixed appear as depletions in the ion signal.

Conformation-specific IR spectra were obtained using resonant ion dip infrared (RIDIR) spectroscopy.[33,34] Tunable infrared radiation from 3300 to 3700 cm^{-1} was produced with a seeded Nd:YAG pumped parametric converter (LaserVision, KTA based, 10 Hz). Typical infrared laser powers were 1−5 mJ/pulse. The IR and UV probe lasers were counter-propagated, spatially overlapped, and temporally separated so the IR laser preceded the probe by 200 ns. The probe laser wavelength was fixed on a transition in the electronic spectrum and the ion signal monitored while the IR was tuned. IR transitions arising from the same ground state level as the probe laser resonance appear as depletions in the ion signal. As in UV−UV hole-burning, active baseline subtraction was employed to compare the difference between IR laser "on" or "off".

2.2. Calculations. In order to ensure a complete search of the conformational space of the molecule, two complementary approaches were taken to identify starting structures for structure optimizations at higher levels of theory. In one approach, a systematic grid of starting structures was generated using the dihedral angles (φ, θ, ψ) along the β-peptide backbone (Figure 1b), using the same procedure as a previous computational study of *N*-acetyl-3-aminobutanoic-acid-*N*′-methylamide (Ac-β^3-hAla-NHMe) from Hofmann et al.[26] Alternatively, a random search was also performed using the Amber force field in MACRO-

(28) Beke, T.; Csizmadia, I. G.; Perczel, A. *J. Comput. Chem.* **2004**, *25*, 285−307.
(29) Beke, T.; Somlai, C.; Perczel, A. *J. Comput. Chem.* **2006**, *27*, 20−38.
(30) Baquero, E. E.; James, W. H.; Choi, S. H.; Gellman, S. H.; Zwier, T. S. *J. Am. Chem. Soc.* **2008**, *130*, 4795−4807.
(31) Seebach, D.; Abele, S.; Gademann, K.; Guichard, G.; Hintermann, T.; Jaun, B.; Matthews, J. L.; Schreiber, J. V. *Helv. Chim. Acta* **1998**, *81*, 932−982.
(32) Shubert, V. A.; Baquero, E. E.; Clarkson, J. R.; James, W. H., III; Turk, J. A.; Hare, A. A.; Worrel, K.; Lipton, M. A.; Schofield, D. P.; Jordan, K. D.; Zwier, T. S. *J. Chem. Phys.* **2007**, *127*, 234315.
(33) Zwier, T. S. *Annu. Rev. Phys. Chem.* **1996**, *47*, 205.
(34) Page, R. H.; Shen, Y. R.; Lee, Y. T. *J. Chem. Phys.* **1988**, *88*, 4621.

MODEL.[35] Lists of starting structures from the two methods were compared and used as the basis for structural optimizations using DFT B3LYP/6-31+G* which employed the GAUSSIAN 03 suite of programs.[36] Since B3LYP calculations do not properly account for dispersion forces, single point MP2/6-31+G* calculations were performed on the optimized DFT structures.[37−40] Also, in an effort to improve our structural assignments, selected structures were reoptimized and the harmonic frequencies recalculated at the RIMP2/aug-cc-pVDZ level of theory.[41−50]

3. Results

The R2PI spectrum of Ac-β^3-hPhe-NHMe in its S_0-S_1 origin region (37380−37590 cm^{-1}) is shown in Figure 2a. This spectrum is dominated by a strong transition at 37431 cm^{-1} which is 100 cm^{-1} lower in frequency than the lowest-frequency conformer origin observed in phenylalanine.[51,52] A UVHB spectrum taken with the hole-burning laser fixed on transition A is shown in Figure 2b. Several of the weak intensity transitions appearing in the UVHB spectrum can be ascribed to vibronic bands of conformer A. Bands labeled B, D, and W do not hole-burn with transition A and hence are due to other species. R2PI spectra taken while monitoring other mass channels indicate that bands at 37465 cm^{-1} (labeled D) and 34576 cm^{-1} (labeled W) are due to the Ac-β^3-hPhe-NHMe dimer and Ac-β^3-hPhe-NHMe·H_2O complex, respectively. These assignments were confirmed by R2PI scans monitoring the relevant cluster mass channels (not shown).

The peak marked B at 37404 cm^{-1} is not due to a cluster and did not vary in intensity with backing pressure relative to A, indicating that it is not a hot band. We shall see shortly that this band has a unique infrared spectrum and is thus ascribable to a second, minor conformer of Ac-β^3-hPhe-NHMe.

The R2PI spectrum of the tyrosine-substituted analogue (Ac-β^3-hTyr-NHMe) is shown over the 35200−35700 cm^{-1} region in Figure 2c). This close analogue of Ac-β^3-hPhe-NHMe was studied in order to test whether the conformational preferences observed in **1** carried over to other close analogues sharing the same β-peptide backbone. The most intense band of Ac-β^3-hTyr-NHMe occurs at 35318 cm^{-1}, 168 cm^{-1} red of the S_0-S_1 origin band of tyrosine.[52−54] Several intense transitions appear just to the high-frequency side of this band, leading to a much more highly congested spectrum than in Ac-β^3-hPhe-NHMe. This increase in the congestion of the spectrum is consistent with the Franck−Condon activity involving several low-frequency vibrations, as occurs in the spectra of tyrosine and tyrosine-substituted polypeptides.[52−54] Figure 2d shows the UV−UV hole-burning of Ac-β^3-hTyr-NHMe taken over the same wavelength region. All transitions to the blue of transition A burn with A, indicating that the entire spectrum is ascribable to a single conformation of Ac-β^3-hTyr-NHMe. Small transitions to the red of the origin of A may be ascribable to a second conformer (analogous to B in Ac-β^3-hPhe-NHMe); however, they were so weak in intensity that they were not pursued further.

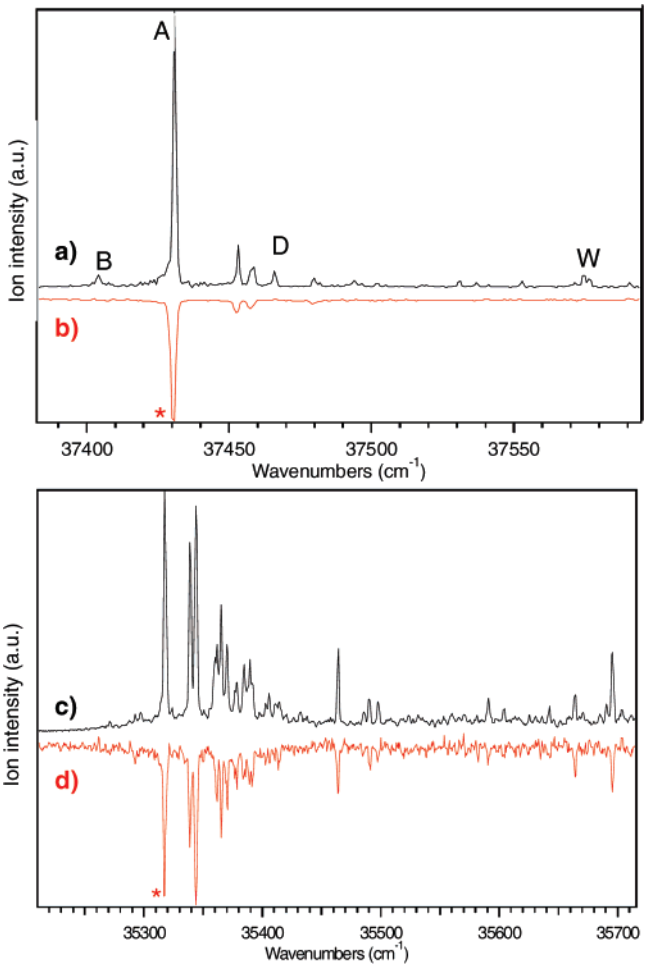

Figure 2. (a) R2PI and (b) UV−UV hole-burning spectrum for Ac-β^3-hPhe-NHMe (**1**). (c, d) Corresponding spectra for Ac-β^3-hTyr-NHMe (**2**). The asterisks denote the transitions used as the hole-burn transition in each case.

RIDIR spectra of Ac-β^3-hPhe-NHMe conformers A and B in the N−H stretch region (3330−3513 cm^{-1}) are shown in Figure 3a,b respectively. As expected, both spectra show two N−H stretch fundamentals associated with the two amide NH groups. Conformer A possesses a sharp NH stretch fundamental at 3488 cm^{-1} and a broadened, more intense transition shifted

(35) Mohamadi, F.; Richards, N. G. J.; Guida, W. C.; Liskamp, R.; Lipton, M.; Caufield, C.; Chang, G.; Hendrickson, T.; Still, W. C. *J. Comput. Chem.* **1990**, *11*, 440−467.
(36) Frisch, M. J.; et al. Revision C.02 ed.; Gaussian, Inc.: Wallingford, CT, 2004.
(37) Zhao, Y.; Truhlar, D. G. *J. Chem. Theory Comput.* **2007**, *3*, 289−300.
(38) van Mourik, T. *Chem. Phys.* **2004**, *304*, 317.
(39) Wodrich, M. D.; Corminboeuf, C.; Schleyer, P. V. *Org. Lett.* **2006**, *8*, 3631−3634.
(40) Perezjorda, J. M.; Becke, A. D. *Chem. Phys. Lett.* **1995**, *233*, 134−137.
(41) RIMP2 Calculations with the Dunning basis set were performed by Dr. Daniel P. Schofield from Prof. Kenneth Jordan's research group, Department of Chemistry, University of Pittsburgh, Pittsburgh, PA 15260.
(42) Bernholdt, D. E.; Harrison, R. J. *Chem. Phys. Lett.* **1996**, *250*, 477.
(43) Dunning, T. H. *J. Chem. Phys.* **1989**, *90*, 1007.
(44) Feyerisen, M.; Fitzgerald, G.; Komornicki, A. *Chem. Phys. Lett.* **1993**, *208*, 359.
(45) Kendall, R. A.; Dunning, T. H.; Harrison, R. J. *J. Chem. Phys.* **1992**, *96*, 6796.
(46) Petersson, K. A.; Dunning, T. H. *J. Chem. Phys.* **2002**, *117*, 10548.
(47) Woon, D. E.; Dunning, T. H. *J. Chem. Phys.* **1993**, *98*, 1358.
(48) Woon, D. E.; Dunning, T. H. *J. Chem. Phys.* **1994**, *100*, 2975.
(49) Woon, D. E.; Dunning, T. H. *J. Chem. Phys.* **1995**, *103*, 4572.
(50) Vahtras, O.; Almlof, J.; Feyerisen, M. W. *Chem. Phys. Lett.* **1993**, *213*, 514.
(51) Snoek, L. C.; Robertson, E. G.; Kroemer, R. T.; Simons, J. P. *Chem. Phys. Lett.* **2000**, *321*, 49−56.
(52) Martinez, S. J.; Alfano, J. C.; Levy, D. H. *J. Mol. Spectrosc.* **1992**, *156*, 421−430.
(53) Cohen, R.; Brauer, B.; Nir, E.; Grace, L.; Vries, M. S. d. *J. Phys. Chem. A* **2000**, *104*, 6351−6355.
(54) Grace, L. I.; Cohen, R.; Dunn, T. M.; Lubman, D. M.; Vries, M. S. d. *J. Mol. Spectrosc.* **2002**, *215*, 204−219.

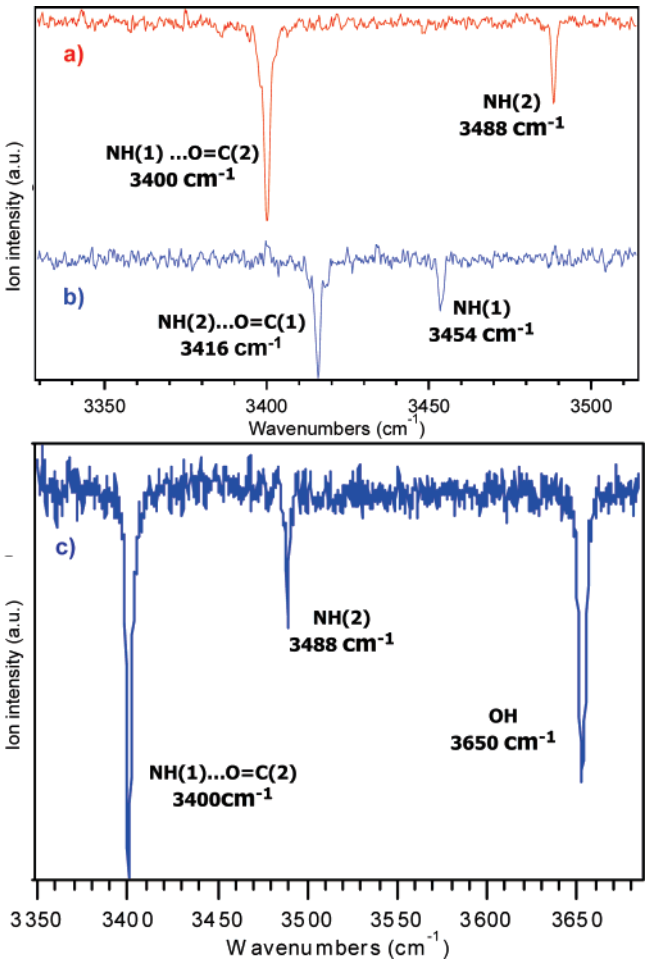

Figure 3. RIDIR spectra in the amide NH stretch region for (a, b) conformers A and B of Ac-β^3-hPhe-NHMe, **1**, respectively, and (c) the sole conformer of Ac-β^3-hTyr-NHMe, **2**.

down in frequency to 3400 cm^{-1}. Both of these characteristics of the 3400 cm^{-1} fundamental indicate that the N−H group responsible for this absorption is involved in a hydrogen bond. Similarly, conformer B shows a free N−H stretch fundamental at 3454 cm^{-1} and a broadened, more intense transition ascribable to a H-bond at 3416 cm^{-1}.

Figure 3c shows the RIDIR spectrum of the single conformer present in Ac-β^3-hTyr-NHMe, taken over the 3330−3680 cm^{-1} region, which includes both amide NH stretch and OH stretch fundamentals. The two fundamentals in the NH stretch region are within 1 cm^{-1} of their values in conformer A in Ac-β^3-hPhe-NHMe, indicating that the most stable backbone conformational preference is maintained upon substitution of Tyr for Phe. This spectrum also shows a band at 3650 cm^{-1} assigned to the O−H stretch of Tyr, appearing within a few cm^{-1} of its value in phenol monomer (3657 cm^{-1}).[55,56]

A preliminary assignment for the H-bonded structures responsible for the IR spectra can be obtained immediately from the spectra. In each case, the spectra contain a 'free' and a H-bonded NH stretch fundamental. Interestingly, the 'free' NH stretch fundamentals of Figure 3a,b are shifted from one another

Table 1. Experimentally determined $S_1 \leftarrow S_0$ Origins and IR Bands of the Two Conformers of Ac-β^3-hPhe-NHMe (**1**) and the Single Conformer of Ac-β3-hTyr-NHMe (**2**)

molecule	ring type	($S_1 \leftarrow S_0$) origins (cm^{-1})	NH(1) stretch (cm^{-1})	NH(2) stretch (cm^{-1})	OH stretch (cm^{-1})	$\Delta\nu$[a] (cm^{-1})
Ac-β^3-hPhe-NHMe (A)	C6	37431	3400	3488		−54
Ac-β^3-hPhe-NHMe (B)	C8	37404	3454	3416		−72
Ac-β^3-hTyr-NHMe	C6	35318	3400	3488	3650	−54

[a] $\Delta\nu$ column represents the frequency shift with respect to the free NH position that occurs upon hydrogen bonding. The free NH frequency position for the C6 and C8 conformers is taken to be 3488 and 3454 respectively.

by 34 cm^{-1}, a larger difference than the H-bonded NH stretches. The shift to 3454 cm^{-1} in Figure 3b could indicate formation of a weak H-bond, such as would occur between an amide NH and the phenyl ring. However, the other possibility is one noted in the introduction, namely, that the frequencies of the free amide NH stretch of the two amide NH groups differ from one another by virtue of their chemically distinct positions in the β-peptide backbone. The structure of Ac-β^3-hPhe-NHMe shows that the N-terminal amide NH(1) is attached to a branched-chain carbon atom, while the C-terminal NH(2) is bonded to a methyl group. According to the previous studies in solution,[25,57,58] NH(1) is thereby predicted to be lower in frequency than NH(2) by about 30−40 cm^{-1}, as observed.

On this basis, we tentatively assign the band at 3454 cm^{-1} to the interior amide group to which the β^3 benzyl side-chain is attached, and the 3488 cm^{-1} transition to the methyl-terminated amide group. H-bonds would then necessarily involve the other amide NH, forming a C6 H-bonded ring in conformer A, and a C8 H-bonded ring in conformer B. Similarly, the only observed conformer of the Tyr analogue would also be assigned to a C6 structure. A summary of these results is shown in Table 1.

4. Calculations

4.1. Conformational Minima. In order to learn more about the structural possibilities available to Ac-β^3-hPhe-NHMe and to refine our assignments, we have used the search and optimization procedure described in Section 2.B to obtain optimized structures, harmonic vibrational frequencies, and infrared intensities for all low-lying minima within 30 kJ/mol of the global minimum on the potential energy surface for Ac-β^3-hPhe-NHMe.

As anticipated, all such conformations of Ac-β^3-hPhe-NHMe contain an NH···O═C H-bond that links an NH of one amide with the carbonyl group of the other. As previously described, the six-membered cycle (C6) is formed when the N−H of the N-terminal amide (NH(1)) is hydrogen bonded to the C═O of the C-terminal amide (CO(1)). Alternatively, the eight-membered cycle (C8) forms when the N−H of the C-terminal amide (NH(2)) hydrogen bonds to the C═O of the N-terminal amide (CO(2)). Different arrangements of the dihedral angles along the β-peptide backbone give rise to distinct C6 and C8 arrangements. Figure 4 shows representative examples of the different types of C6 and C8 structures which can be formed. These structures differ from one another

(55) Ebata, T.; Watanabe, T.; Mikami, N. *J. Phys. Chem.* **1995**, *99*, 5761−5764.
(56) Tanabe, S.; Ebata, T.; Fujii, M.; Mikami, N. *Chem. Phys. Lett.* **1993**, *215*, 347−352.
(57) Fillaux, F.; Loze, C. *Biopolymers* **1972**, *11*, 2063−2077.
(58) Aubry, A.; Cung, M. T.; Marraud, M. *J. Am. Chem. Soc.* **1985**, *107*, 7640−7647.

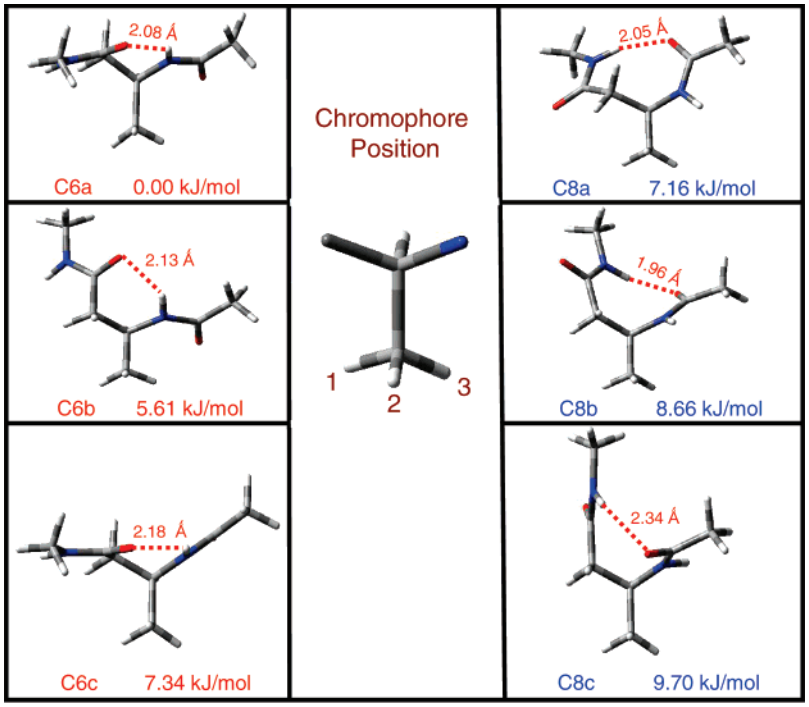

Figure 4. Representative structures (DFT B3LYP/6-31+G*). (Left/right) Three lowest energy C6/C8 chain arrangements. The phenyl ring has been removed for clarity. (Center) Three possible chromophore positions for the phenylalanine or tyrosine side chain on the β^3 carbon.

Table 2. Key Spectroscopic and Structural Data Calculated for the Low-Lying Minima of Ac-β^3-hPhe-NHMe, **1**, at the Indicated Level of Theory

conformer	φ^a	θ^a	ψ^a	O···H distance (Å)	calculated NH(1)[b] stretch (cm^{-1})	calculated NH(2)[b] stretch (cm^{-1})	ΔE_0 DFT[c] (OPT) (kJ/mol)	ΔE_0 MP2[d] (SP) (kJ/mol)	ΔE_0 RIMP2[e] (OPT) (kJ/mol)	fractional[f] population behind nozzle
extended(2)	−118.3	17.3	143.0	–	*3455.55*	*3489.06*	36.87	45.58	–	–
C6a(1)	−147.7	−60.8	−134.9	2.08	3411.18	*3490.11*	0.00	0.00	0.00	0.445
C6b(1)	−161.4	53.0	108.8	2.13	3397.93	*3488.33*	5.63	8.32	11.55	0.032
C8a(3)	−70.0	132.6	−73.9	2.05	*3462.11*	3373.86	7.16	7.29	11.34	0.033
C6c(3)	−112.3	−63.8	−148.0	2.18	3443.6 9	*3488.06*	7.34	9.85	–	0.014
C8b(1)	−109.7	67.7	11.3	1.96	*3463.88*	3348.17	8.66	7.57	13.60	0.035
C8c(3)	50.1	53.0	−108.4	2.34	*3480.10*	3437.03	9.70	4.31	–	0.176
C8b(2)	−109.5	68.4	10.5	1.99	*3453.79*	3361.00	9.77	8.55	7.49	0.060
C8d(3)	−54.4	−49.6	105.5	2.31	*3448.24*	3434.51	10.65	5.76	–	0.064
C8a(2)	−71.3	138.7	−74.1	2.22	*3452.87*	3390.44	11.12	8.70	7.41[g]	0.027
C6b(2)	−161.7	52.6	110.5	2.12	3401.95	*3491.62*	12.13	11.96	–	0.007
C6a(2)	−148.2	−48.8	−132.6	1.98	3379.55	*3487.29*	14.18	4.74	–	0.101
C8a(1)	−78.2	132.7	−49.5	1.97	*3462.15*	3343.05	16.11	18.10	–	0.002
C8e(3)	58.0	−120.2	82.4	1.94	3481.48	3373.48	20.52	17.28	–	0.003

[a] Dihedral angles along β-peptide chain (for definition, see text and Figure 1b). Different dihedral arrangements are included in the conformer labeling by the letters a−c for C6 conformers and a−e for C8 conformers. C6 (a, b, c) correspond to structures labeled B1, B5, B4 by Hofman.[26] C8 (a,b,c,d,e) correspond to structures labeled B2, B6, B3′, B3, B2′ by Hofman.[26] [b] Calculated NH stretches for NH(1) and NH(2) along the β-peptide chain (free NH stretches are italic). [c] Zero point corrected energies of optimized structures at DFT/6-31+G* level of theory. [d] Single point, zero point corrected energies at MP2/6-31+G* level of theory of DFT/6-31+G* structures (zero point correction done with DFT harmonic frequencies). [e] Zero point corrected energies of selected structures optimized at RIMP2 level. [f] Fractional population of conformers behind the nozzle calculated by adding the free energy available at the stagnation temperature (453 K) to the zero point corrected MP2 single point energies. [g] C8a(2) Experience a major structural change upon RIMP2 optimization.

in the relative orientation of the peptide groups involved in the H-bond created by different dihedral angles in the β-peptide backbone. The different ring types are labeled a−c for C6 conformers and a−e for C8 conformers in Table 2. The torsional dihedral angles associated with the structures listed in Table 2 have been previously observed in computational work by Hofman and others.[26−29] In addition, for each β-peptide backbone structure, there are three distinct positions, numbered 1 through 3, for the phenyl ring. In some cases, not all three phenyl ring positions give stable minima, producing five C6 structures and eight C8 structures with energies within 20 kJ/mol of the global minimum. The key dihedral angles and relative energies of the lowest energy (<20 kJ/mol) optimized structures are listed in Table 2.

4.2. Vibrational Frequencies. In order to assess whether the calculations predict a difference in frequency for the two amide NH stretch modes, a completely extended structure for the β-peptide backbone was optimized and the free amide NH stretch fundamentals calculated for branched-chain and methyl-terminated amide NH groups. As can be seen from Table 2, the methyl-terminated free NH(2) stretch has a calculated frequency of 3490 cm^{-1} (after scaling by 0.96 to match the

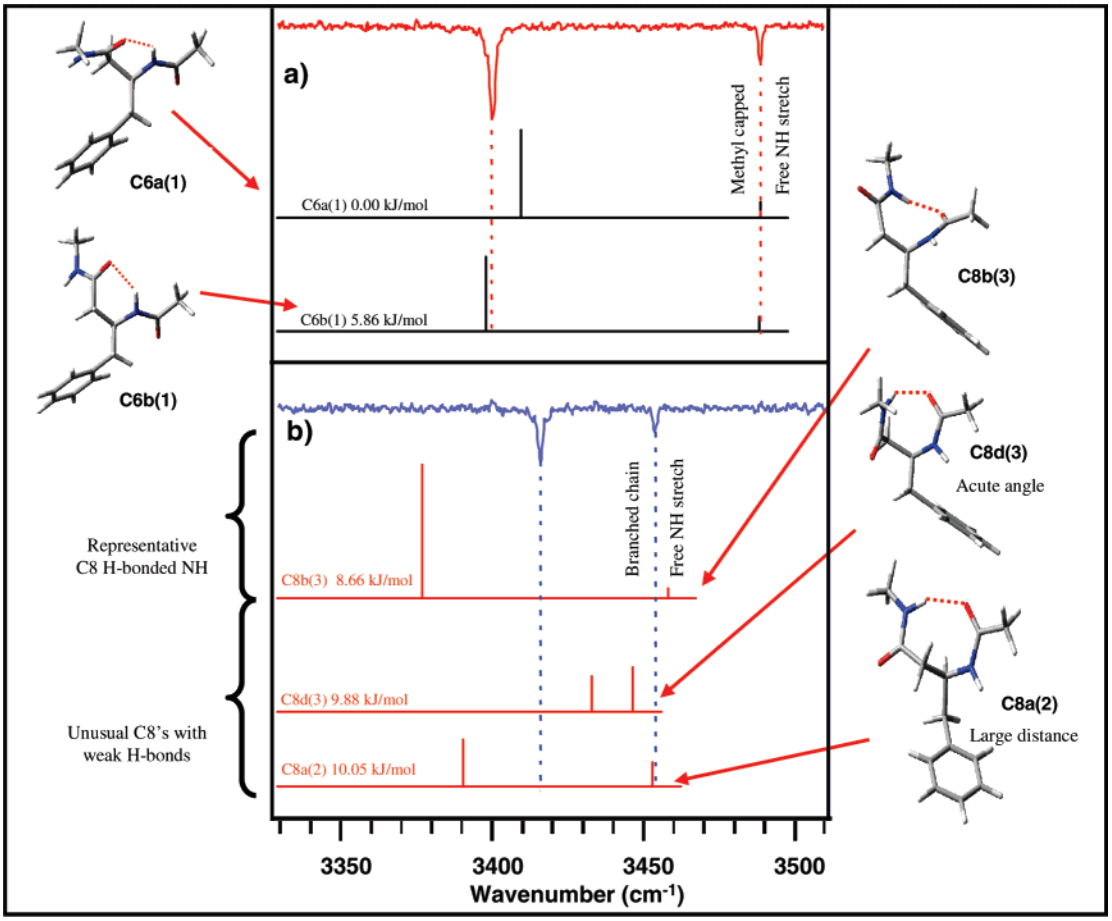

Figure 5. (a, b) Top traces: RIDIR spectra of conformer A and B of Ac-β^3-hPhe-NHMe, **1** in the NH stretch region. The stick diagrams below the experimental spectra are calculated, scaled harmonic vibrational frequencies, and infrared intensities (DFT B3LYP/6-31+G*) of representative C6 (top) and C8 (bottom) β-peptide backbone arrangements. Structures on both sides are connected to their calculated IR spectrum. The C8d(3) and C8a(2) are structures with unusually weak H-bonds due to an acute angle or large distance of the C8 H-bond.

calculated highest-frequency free NH to the one observed experimentally), while the branched-chain free NH(1) stretch is 30 cm^{-1} lower in frequency. Furthermore, this difference in frequency is seen to be a general feature of all conformational minima. Whenever the methyl terminated chain NH(2) is free, its frequency is in a range from 3487 to 3490 cm^{-1}, while the branched-chain free NH(1) frequency is predicted to fall somewhere in the range from 3448−3481 cm^{-1}. The stick spectra shown in Figure 5a illustrate this for a representative set of C6 and C8 structures. Note that the two regions are nonoverlapping, and hence diagnostic of which NH group is free. Therefore, the calculations support the assignment of conformer A to a C6 structure and conformer B to a C8 structure.

The calculations also predict a close match between experiment and calculation in the frequencies and relative infrared intensities of the H-bonded NH stretch modes of the C6 conformers. The full set of calculated frequencies are given in Table 2, while Figure 5a shows the calculated spectra of the lowest two C6 conformers, which differ in the type of C6 ring (a vs b, Figure 2) but share the same phenyl ring position (position 1, Figure 2). We cannot distinguish between these two C6 conformations based on the infrared spectra, but the fact that C6a(1) is calculated to be lowest in energy at all levels of theory supports this assignment.

The comparison between experiment and theory is much less satisfying for the H-bonded NH stretch of conformer B, the C8 conformer. A survey of Table 2 indicates that the great majority of C8 conformers have calculated, scaled frequencies for the H-bonded NH stretch that are lower in frequency than the H-bonded NH stretch of the C6 conformers, at odds with experiment. The stick spectrum of the calculated, lowest-energy C8 conformer is included in Figure 5b, illustrating this fact. This led us to search carefully for C8 conformers with a weaker H-bond, leading to a smaller H-bonded NH stretch frequency shift. The structures and calculated stick spectra for two such C8 conformers are shown in Figure 5b. The C8d(3) conformer has a highly unusual C8 ring (labeled 'd') that forms an NH···O=C H-bond in which the two amide planes are at an acute angle that leads to a strongly bent H-bond, which is thereby weakened. The C8a(2) conformer has an unsually large H-bond distance caused by the presence of the phenyl ring in the 2 position, where both branches of the β-peptide backbone are in gauche positions relative to the phenyl ring. The NH(1) group is positioned so that it can interact with the phenyl ring to form a stabilizing NH···π interaction, thereby opening up the C8 ring.

Because DFT is known[37−40] not to account for dispersive interactions properly, the C8a(2) structure and several others were optimized at the RIMP2/aug-cc-pVDZ level of theory. While most structures showed only modest shifts in relative energies or vibrational frequencies, the C8a(2) structure opened up the C8 ring in order to accommodate a stronger dispersive interaction between the NH(1) group and the π cloud, leading

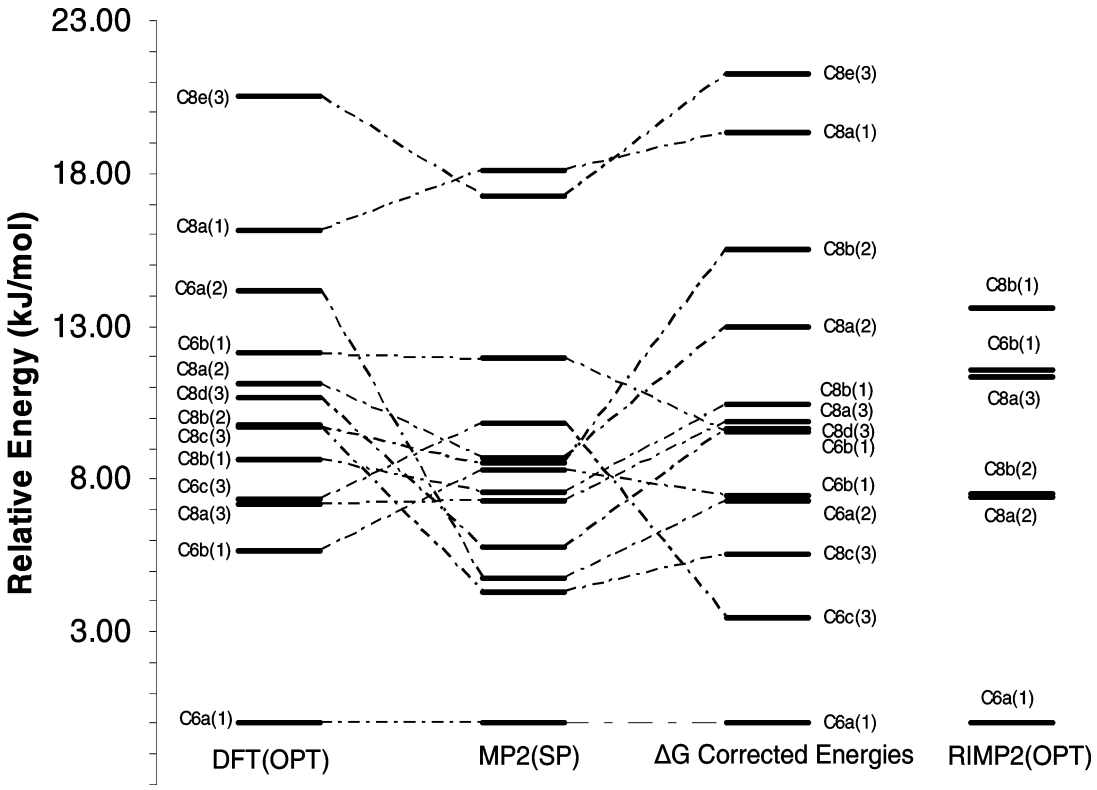

Figure 6. Relative energies for Ac-β^3-hPhe-NHMe (**1**) conformers at different levels of theory. The structural details and quantitative energies for each structure are given in Table 2. DFT(OPT): Fully optimized structures computed using DFT B3LYP/6-31+G*. MP2(SP): Single point MP2/6-31+G* calculations at the optimized DFT geometries. ΔG corrected energies: Relative free energies at the preexpansion temperature (453 K) based on the MP2(SP) relative energies. All calculations are zero point corrected utilizing DFT calculated harmonic frequencies. RIMP2(OPT): Fully optimized relative energies for a select set of structures at the RIMP2/aug-cc-pVDZ level of theory.

to a significant shift of the H-bonded NH stretch toward higher frequency. In fact, the RIMP2 calculations still do not match up with experiment quantitatively, in this case predicting that the C8 H-bond is essentially broken. This result highlights the sensitivity of this unique C8 H-bond to the proper description of dispersive interactions.

On the basis of these calculations, we make a tentative assignment of the C8a(2) structure as the observed C8 conformer. If correct, the overcompensation of the RIMP2 calculations must be attributed to this level of theory overemphasizing dispersive interactions, as has been noted previously.[59,60] We anticipate that calculations carried out at higher levels of theory would lead to vibrational frequencies somewhere between the DFT and RIMP2 'limits', in keeping with experiment.

5. Discussion

5.1. Conformational Preferences and Infrared Spectral Signatures. A primary finding of the present study is that the spectra of the expansion-cooled, isolated β-peptides Ac-β^3-hPhe-NHMe and Ac-β^3-hTyr-NHMe are dominated by transitions assigned to a C6 structure, forming a six-membered, H-bonded cycle between NH(1) and CO(2). A second, minor conformer has been assigned to a C8 structure, with an intramolecular H-bond formed between NH(2) and CO(1). In the present circumstances, it seems likely that the relative intensities of the S_0-S_1 origins are a reasonable measure of their relative populations. Since neither conformer shows significant Franck−Condon activity in low-frequency vibrations, we do not anticipate large differences in the Franck−Condon factors or oscillator strengths associated with the origin transitions. If these differences are small, the observed intensity ratio (22:1) indicates that about 95% of the population of Ac-β^3-hPhe-NHMe is in the C6 conformer and the remaining 5% in the C8 conformer.

A first question that should be addressed, then, is why this preference for C6 over C8 structures exists. Figure 6 presents an energy level diagram that summarizes the relative energies of the low-energy conformers of Ac-β^3-hPhe-NHMe calculated at the DFT B3LYP/6-31+G* level of theory. The figure also includes the results of MP2 single point calculations at the B3LYP-optimized geometries, and RIMP2/aug-cc-pVDZ optimizations on a select subset of structures. All levels of theory predict C6a(1) as the lowest energy structure. Above this, C6 and C8 conformers are close in energy and intermingled with one another.

Figure 6 also shows free-energy corrected relative energies of the same conformers computed at the temperature of the sample prior to supersonic expansion (453 K). The free energy correction was computed using harmonic vibrational frequencies from the B3LYP/6-31+G* calculations. C6a(1) remains the most populated conformer and thereby a likely candidate for the observed C6 conformer. However, C6b(1) displays a better match between the experimental and calculated H-bonded NH stretch. Our confidence in the accuracy of the calculated vibrational frequencies or relative energies/fractional populations is insufficient to make a firm assignment on the basis of either one.

(59) Hopkins, B. W.; Gregory, S. T. *Chem. Phys. Lett.* **2005**, *407*, 362−367.
(60) Levy, J. B.; Martin, N. H.; Hargittai, I.; Hargittai, M. *J. Phys. Chem. A* **1998**, *102*, 274−279.

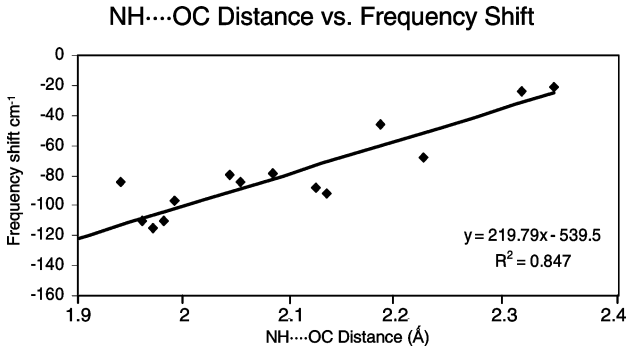

Figure 7. Calculated shifts of the scaled, H-bonded C6 or C8 NH stretch vibrational frequencies (in cm^{-1}) of Ac-β^3-hPhe-NHMe (**1**) versus NH····OC distance. The zero of the relative frequency scale is the scaled frequency of the free NH stretch of **1** at 3489 cm^{-1} for C6 and 3458 cm^{-1} for C8 conformers.

The dominance of the C6 conformer (both in the Phe and Tyr analogues) occurs despite the fact that even the weak H-bond formed in the observed C8 conformer is stronger than that in the C6 conformer, based on the magnitude of the frequency shift induced by the intramolecular H-bond, which was greater for the C8 (-72 cm^{-1}) than C6 (-54 cm^{-1}). As Figure 7 shows, the frequency shift is inversely correlated with the H-bond distance, another oft-used measure of the strength of the H-bond.

This counterintuitive result is in keeping with previous deductions[24] that observed conformational preferences represent a delicate balance between H-bond strength, ring strain, and other, less-specific stabilizing factors such as dispersive interactions. This result is driven home by the fact that the calculations show a much wider spread in energies among C6 or C8 conformers than separates the two families (Figure 6).

Given the results of Figure 6, it is also intriguing that only one C6 and one C8 conformer are observed experimentally. Table 2 lists the fractional populations in the preexpansion gas mixture predicted by the calculations. The average internal energy of predicted conformers is calculated at the preexpansion sample temperatures (453 K) using unscaled B3LYP frequencies and single point MP2 energies at the DFT-optimized geometries. The energy distribution obtained from this calculation was used to determine the fractional population of the predicted conformers. These populations are much more broadly distributed than experiment, indicating either that the calculated preexpansion populations are not accurate, or that significant transfer of population into the lowest energy C6 and C8 conformational wells occurs during the expansion cooling. Since one of the goals of these studies is to provide benchmark data for calculations, it is important for calculations of these quantities to be carried out at higher levels of theory until convergence is reached.

It will also be important to learn more about the barriers that separate the conformational isomers listed in Figure 6. Several past studies on other flexible biomolecules have concluded that the downstream populations are representative of the preexpansion populations, as would occur if collisional cooling were fast compared to isomerization.[61−68] However, in cases where these barriers are small compared to the average internal energy available to the molecules, collisional cooling could redistribute the population during the early portion of the expansion, thereby funneling the population toward the lowest energy conformers.[62,68−72] From an experimental standpoint, this calls for direct experimental measures of the barriers separating the isomers, using either SEP or IR population transfer spectroscopy.[73−75] Since calculations at both DFT and RIMP2 levels of theory consistently predict the C6a(1) structure to be most stable, this conformer would be the natural recipient of population from other conformers during the cooling process. It is less clear why a single C8 conformer is also observed, despite the fact that several other structures, both C6 and C8, are calculated to be lower in energy than the weakly H-bonded C8 conformer which is most consistent with the experimental infrared spectrum. If the potential energy surface divides into two subspaces involving C6 and C8 conformers with large barriers separating them, then collection of population from the C8 family into a single well is plausible. Ultimately, a full exploration of the barriers separating minima (leading to a disconnectivity diagram)[76,77] and simulation of the expansion cooling will be needed before a quantitative account of the observed populations is possible.

Another primary result of the present study is the determination of the amide NH stretch infrared spectral signatures for the observed C6 and C8 conformers under jet-cooled, isolated conditions. Interestingly, the key to our assignment is the free amide NH stretch fundamental rather than the H-bonded NH stretch. One might have thought that the size of the H-bonded ring would present the most obvious and characteristic difference in the NH stretch region, which is exquisitely sensitive to its H-bonding environment. However, the H-bonded NH stretch transitions of conformers A and B are within 20 cm^{-1} of one another, making it difficult to secure an assignment as C6 or C8 on this basis alone.

5.2. Comparison with Solution. One interesting comparison that is worth making is the one between the conformation-specific infrared spectra obtained in the present study and the infrared spectrum of the same molecule in room-temperature, nonpolar solution.

Several previous studies of the conformational preferences of closely analogous molecules have been carried out. Those most relevant to the present work are the studies of β-peptides by Marraud et al.[25] and Dado and Gellman.[8] The study of **3** and **4** by Marraud et al. was mentioned earlier as the basis of the assignment of the NH group responsible for a given free

(61) Macleod, N. A.; Simons, J. P. *Phys. Chem. Chem. Phys.* **2004**, *6*, 2878−2884.
(62) Felder, P.; Gunthard, H. H. *Chem. Phys.* **1982**, *71*, 9−25.
(63) Fraser, G. T.; Suenram, R. D.; Lugez, C. L. *J. Phys. Chem. A* **2001**, *105*, 9859−9864.
(64) Kaczor, A.; Reva, I. D.; Proniewicz, L. M.; Fausto, R. *J. Phys. Chem. A* **2006**, *110*, 2360−2370.
(65) Kim, D.; Baer, T. *Chem. Phys.* **2000**, *256*, 251−258.
(66) Pitts, J. D.; Knee, J. L.; Wategaonkar, S. *J. Chem. Phys.* **1999**, *110*, 3378−3388.
(67) Reva, I. D.; Stepanian, S. G.; Adamowicz, L.; Fausto, R. *Chem. Phys. Lett.* **2003**, *374*, 631−638.
(68) Ruoff, R. S.; Klots, T. D.; Emilsson, T.; Gutowsky, H. S. *J. Chem. Phys.* **1990**, *93*, 3142−3150.
(69) Basu, S.; Knee, J. L. *J. Phys. Chem.* A **2001**, *105*, 5842−5848.
(70) Godfrey, P. D.; Brown, R. D.; Rodgers, F. M. *J. Mol. Struct.* **1996**, *376*, 65−81.
(71) McCoustra, M. R. S.; Hippler, M.; Pfab, J. *Chem. Phys. Lett.* **1992**, *200*, 451−458.
(72) Miller, T. F.; Clary, D. C.; Meijer, A. *J. Chem. Phys.* **2005**, *122*.
(73) Clarkson, J. R.; Baquero, E.; Shubert, V. A.; Myshakin, E. M.; Jordan, K. D.; Zwier, T. S. *Science* **2005**, *307*, 1443−1446.
(74) Clarkson, J. R.; Baquero, E.; Zwier, T. S. *J. Chem. Phys.* **2005**, *122*.
(75) Dian, B. C.; Clarkson, J. R.; Zwier, T. S. *Science* **2004**, *303*, 1169−1173.
(76) *Advances in Chemical Physics*; Wales, D. J.; Doye, P. K.; Miller, M. A.; Mortenson, P. N.; Walsh, T. R., Eds.; Wiley: New York, 2000; Vol. 115.
(77) Becker, O. M.; Karplus, M. *J. Chem. Phys.* **1997**, *106*, 1495.

amide NH stretch in branched-chain versus unbranched-chain amides. In CCl_4 solution, they observed a set of four bands in the amide NH stretch region, which were attributed to a mixture of C6 and C8 structures, with the former possessing a free NH at 3469 cm^{-1} and a H-bonded NH stretch at 3393 cm^{-1}, while the latter had its analogous bands at 3437 and 3340 cm^{-1}.

Dado and Gellman carried out a complementary study of the β-diamides **5**−**7**, shown below.

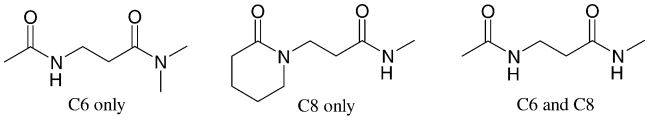

5 **6** **7**

By appropriate substitution, diamides **5** and **6** are capable of forming only C6 or C8 H-bonded rings, respectively, while **7** can form both. In dilute CH_2Cl_2 solution, amide NH stretch IR spectra of **5** in CH_2Cl_2 showed a single band peaked at 3440 cm^{-1}, taken as evidence that no C6 H-bonded rings were present, while **6** showed two bands at 3455 and 3295 cm^{-1}, signaling the presence of and competition between non-H-bonded structures and those containing C8 rings. The band at 3295 cm^{-1}, attributed to the C8 ring, is much lower in frequency than the one observed in the gas-phase RIDIR spectrum of conformer B of **1** (3416 cm^{-1}). The shift to higher frequency in the gas-phase experiment cannot be ascribed solely to solvent effects but points to the fact that the C8 conformer observed in the jet has an unusually weak H-bonded arrangement. Finally, in **7**, a single peak at 3453 cm^{-1} was assigned to non-H-bonded NH groups, indicating that neither C6 nor C8 rings were substantially populated in room temperature solution.

This body of results illustrates how sensitive the conformational preferences of small β-peptides are to substitution and to solvent. As a result, we decided to record solution-phase infrared spectra of **1**, with its phenylalanine substituent, for direct comparison with the jet-cooled, isolated molecule results.

Figure 8 presents this comparison. The room-temperature, solution-phase spectrum of a 1 mM solution of **1** in CH_2Cl_2 solvent is shown in the figure, shifted to higher frequency by 35 cm^{-1} in order to match the free amide NH stretch transitions in solution with the C6 gas-phase result. The solution-phase spectrum shows a shoulder 30 cm^{-1} below the main free amide NH stretch transition which is ascribable to the free amide NH stretch transition of NH(1), the interior branched-chain NH group. Below this shoulder, the absorption tails off toward lower frequency, with no further well-defined peaks.

In the isolated molecule, the H-bonded NH stretch fundamentals of both conformers occur within the low-frequency wing in the solution-phase spectrum. As a result, we ascribe some or all of the intensity of the low-frequency wing to C6 or C8 rings. The lack of a well-defined band in this region probably arises from broadening of the H-bonded NH stretch in room-temperature solution, due to modulation of the strength of the C6 H-bonded ring by the solvent and internal energy effects. The integrated intensity of this low-frequency wing is only about 50% of the methyl-terminated and branched free NH, indicating that the majority of molecules in solution are not H-bonded.

By contrast, the free amide NH stretch bands can have contributions both from non-H-bonded and H-bonded structures,

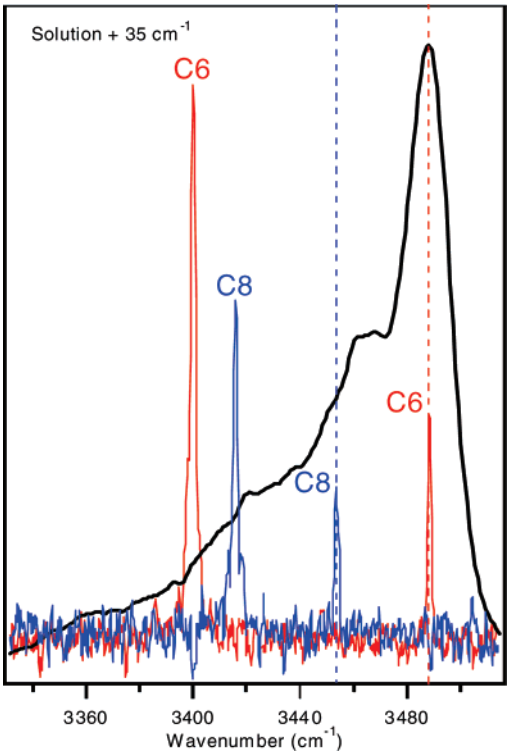

Figure 8. Comparison of single-conformation amide NH stretch infrared spectra obtained in the present study to solution-phase FT-IR spectra of a 1 mM solution of Ac-β³-hPhe-NHMe (**1**) in CH_2Cl_2. Bands are labeled A C6 and B C8 for the two observed conformers of **1**. The solution-phase trace is shifted 35 cm^{-1} to higher frequency to match the free NH stretch band of A in the isolated molecule spectra.

since the free NH stretch frequency depends primarily on local chemical structure and not its chain conformation. As a result, the intensity ratio of the two free NH peaks reflects the total number of free NH groups of each type in solution, quantitatively so if the two free NH stretch modes have identical oscillator strengths. In the limit that no intramolecular H-bonded rings are formed, the spectrum would then consist of two free NH stretch peaks of roughly equal intensity. We therefore interpret the observed large intensity of the methyl-terminated free NH in the spectrum as a reflection of the dominance of non-H-bonded and C6 H-bonded rings in solution.

6. Conclusions

In this study, double resonance spectroscopy has been used to record the infrared and ultraviolet spectra of single conformations of two model β-peptides, Ac-β³-hPhe-NHMe and Ac-β³-hTyr-NHMe. The characteristic amide NH stretch frequencies for both free amide NH and H-bonded amide NH will serve as useful benchmarks for analogous studies of longer β-peptide chains. In particular, the adjoining paper describes a study of β-peptides Ac-β³-hAla-β³-hPhe-NHMe and Ac-β³-hPhe-β³-hAla-NHMe which builds directly upon the present work.

Acknowledgment. E.E.B., W.H.J., and T.S.Z. gratefully acknowledge support for this work from the National Science Foundation (CHE-0551075). The authors also gratefully acknowledge Daniel Schofield and Kenneth D. Jordan from the University of Pittsburgh for optimizing the structures of a select subset of conformational minima of Ac-β³-hPhe-NHMe at the RIMP2/aug-cc-VDZ level of theory. They also gratefully

acknowledge V. Alvin Shubert for helping set up systematic explorations of the conformational phase space of these molecules. S.H.G. and S.H.C. acknowledge support under NSF CHE-0551920. S.H.C. was supported in part by the Samsung Scholarship Foundation.

Supporting Information Available: Complete ref 36. This material is available free of charge via the Internet at http://pubs.acs.org.

JA078271Y